Published in final edited form as:
Transplantation. 2011 March 27; 91(6): 615–623. doi:10.1097/TP.0b013e3182094a33.

Unique cellular and mitochondrial defects mediate FK506-induced islet β-cell dysfunction

Nassir Rostambeigi[1], **Ian R. Lanza**[1], **Petras Dzeja**[2], **Michael C. Deeds**[3], **Brian A. Irving**[1], **Honey V. Reddi**[1], **Pranathi Madde**[1], **Song Zhang**[2], **Yan W. Asmann**[4], **Jarett M. Anderson**[3], **Jill M. Schimke**[1], **K. S. Nair**[1], **Norman L. Eberhardt**[1,5], and **Yogish C. Kudva**[1]

[1]Department of Medicine, Division of Endocrinology, Mayo Clinic, Rochester, MN 55902

[2]Cardiovascular Disease, College of Medicine, Mayo Clinic, Rochester, MN 55902

[3]Human Cell Therapy Laboratory, Mayo Clinic, Rochester, MN 55902

[4]Biomedical Statistics and Informatics, Mayo Clinic, Rochester, MN 55902

[5]Department of Biochemistry and Molecular Biology, Mayo Clinic, Rochester, MN 55902

Abstract

Objective—Determine biological mechanisms involved in post transplantation diabetes mellitus caused by the immunosuppressant FK506.

Methods—INS-1 cells and isolated rat islets were incubated with vehicle or FK506 and harvested at 24 hr intervals. Cells were assessed for viability, apoptosis, proliferation, cell insulin secretion and content. Gene expression studies by microarray analysis, qPCR and motifADE analysis of the microarray data identified potential FK506-mediated pathways and regulatory motifs. Mitochondrial functions, including cell respiration, mitochondrial content and bioenergetics were assessed.

Results—Cell replication, viability, insulin secretion, oxygen consumption, and mitochondrial content were decreased ($p < 0.05$) 1.2-, 1.27-, 1.77-, 1.32-, and 1.43-fold, respectively after 48 hr FK506 treatment. Differences increased with time. FK506 (50 ng/ml) and Cyclosporine A (800 ng/ml) had comparable effects. FK 506 significantly decreased mitochondrial content and mitochondrial bioenergetics and showed a trend towards decreased oxygen consumption in isolated islets. Cell apoptosis and proliferation, mitochondrial DNA copy number and ATP/ADP ratios were not significantly affected. Pathway analysis of microarray data showed FK506 modification of pathways involving ATP metabolism, membrane trafficking and cytoskeleton

Corresponding Author: Yogish C. Kudva, Department of Medicine, Division of Endocrinology, Mayo Clinic, 200 First Street SW, Rochester, MN 55905, Phone: 507 284 3964 Fax: 507 284 5745 Kudva.yogish@mayo.edu.

Nassir Rostambeigi: research design, performance of the research, writing of the paper, performance of the research, data analysis
Ian R Lanza: performance of the research, writing of the paper, data analysis
Petras Dzeja: performance of the research, writing of the paper
Micheal Deeds: performance of the research
Brian A. Irving: performance of the research, writing of the paper
Honey Reddi: performance of the research
Pranathi Madde: performance of the research
Song Zhang: performance of the research
Yan W. Asmann: performance of the research, writing of the paper, data analysis
Jarett M. Anderson: performance of the research, writing of the paper
Jill M Schimke: performance of the research, writing of the paper
K S Nair: performance of the research, writing of the paper
Norman L Eberhardt: research design, performance of the research, writing of the paper, data analysis
Yogish C Kudva: research design, performance of the research, writing of the paper, data analysis

remodeling. PGC1-α mRNA was down-regulated by FK506. MotifADE identified nuclear factor of activated T-cells (NFAT), an important mediator of β cell survival and function, as a potential factor mediating both up- and down-regulation of gene expression.

Conclusions—At pharmacologically relevant concentrations FK506 decreases insulin secretion and reduces mitochondrial density and function without changing apoptosis rates, suggesting that post transplantation diabetes induced by FK506 may be mediated by its effects on mitochondrial function.

Introduction

With the increasing utilization of solid organ transplantation (SOT) and improved postoperative survival (1), adverse effects of long term immunosuppression, especially post-transplantation diabetes mellitus (PTDM) are concerning (2). PTDM is an adverse effect of calcineurin inhibitors such as Tacrolimus (FK506) and Cyclosporine A (CsA) with FK506 being significantly more diabetogenic (2–4). We showed that PTDM is associated with high cumulative incidence of mortality and cardiovascular events (5). Although, the effect of FK506 is reversible after the withdrawal of the agent in animal studies (6), the chronic need for immunosuppression in patients makes its continuous usage necessary.

Calcineurin and downstream signaling pathways are ubiquitous molecules with biologic relevance in multiple tissues. Calcineurin is a cytoplasmic molecule consisting of regulatory (Cnb1) and phosphatase units. FK506, after binding to its cytoplasmic receptor (FKBP12.6), inhibits Cnb1 and downstream pathways. Although calcineurin may affect several other pathways, one of the major cellular pathways affected is cytoplasmic Nuclear Factor of Activated T-cells (NFATc). The phosphatase subunit of calcineurin dephosphorylates NFATc, resulting in nuclear translocation and transcription of specific genes leading to secretion of insulin and proliferation of β cells (7).

The development of FK506-induced PTDM may be multifactorial: (1) insulin secretion impairment consequent to either decreased insulin expression or lower secretory capacity in β cells (8–11); (2) altered glucokinase function, lowering the efficiency of glucose-induced insulin secretion (12); (3) increased apoptosis in the islets; and (4) other uncharacterized effects. FK506 has also been shown to induce shrinkage and damage of islets on electron microscopic examination of pancreas allografts (13, 14). CsA was shown to result in apoptosis of β cell lines (15) but these effects were demonstrated at concentrations about 15 times higher than those achieved in humans (16). Finally, NFATc has been shown to be associated with decreased islet mass and diabetes mellitus in a tissue specific knock-out mouse model (11).

Insulin secretion results from an increase in ATP/ADP ratio (due to glucose metabolism) and Ca^{2+} flux across cell membrane and ER. For the Ca^{2+} flux to occur, ATP sensitive K^{+} channels must be blocked (17, 18) and mitochondrial function becomes critical because of its central role in ATP production. To further evaluate the intracellular mechanisms involved in the pathogenesis of PTDM, we performed experiments with the rat insulinoma cell line INS-1 and isolated rat islets. We established *in vitro* conditions using FK506 doses equivalent to peak therapeutic concentrations. Gene expression and mitochondrial studies indicated that FK506 treatment was associated with impairment of pathways involving ATP metabolism and NFATc, altered mitochondrial oxygen consumption and reduced mitochondrial density. Our data suggest that FK506-induced impairment of mitochondrial function may play a major role in the development of PTDM.

Methods

Cell Culture

INS-1 cells were provided by Professor Chris Rhodes (University of Chicago, Illinois). INS-1 cells were incubated in RPMI1640 (Invitrogen, Carlsbad, CA), 10% fetal bovine serum (Hyclone, Logan, UT), sodium pyruvate (Sigma-Aldrich, St. Louis, MO), mercaptopurine (Bio-Rad Laboratories, Hercules, CA), and HEPES (Invitrogen) at 37°C in 5% CO_2. Cell numbers were determined with a hemocytometer. Multiple concentrations of FK506 monohydrate (Sigma-Aldrich) at 15, 50 and 150 ng/ml were added to cells 24 hr after plating. FK506 was dissolved in dimethyl sulfoxide (DMSO, 99.5%, Sigma-Aldrich). DMSO at an identical concentration was used as control in all experiments.

Rat islet studies

Male Wistar Hannover GALAS rats (Taconic, Hudson, NY) weighing 250–300 grams were used as donors and islets isolated using a modified version of a previously published rat islet isolation protocol (19). Briefly, islets were isolated using a discontinuous Dextran based gradient. Islets were hand picked under magnification using a modified 200 μL pipette tip attached to a threaded syringe (Hamilton Company, Reno, NV). Islets were cultured under the identical conditions used for INS-1 cells except that media containing FK506 was changed every 24 hr.

Cell Viability Assay

INS-1 cells were plated in 12-well plates at 75,000 cells per well. At the specified times, cells were incubated for 30 min in MTT reagent (Sigma Chemical Co.) (diluted in phenol free 20% RPMI) at 37°C and absorbance determined using a micro-plate reader (Hitachi U-2000, Tokyo, Japan).

Apoptosis Assay

INS-1 cells (1.5×10^6) were seeded in 10 cm cell culture dishes. At 24, 48 and 72 hr cells were harvested and tested by Annexin-V binding (TACS Annexin V kit, Trevigen Inc. Gaithersburg, MD). Cells were incubated with Phycoerythrin (PE, Invitrogen) and Annexin-V binding assessed by flow cytometry (Becton Dickinson Immunocytometry Systems, San Jose, CA). Tunicamycin served as a positive control.

Insulin Measurement

INS-1 cells (1.5×10^6) were seeded in 10 cm cell culture dishes and incubated up to 72 hr with supernatant media and collected every 24 hr for insulin measurement. Cells were lysed by subjecting to three freeze-thaw cycles and the cells dissolved in M-PER (Thermo Scientific, Rockford, IL). Insulin was measured by ELISA (Crystal Chem ELISA kit, Downers Grove, IL, USA).

Microarray Analysis

Total RNA was extracted from samples cultured in vehicle or FK506 (50 ng/ml) for 48 hr using Trizol (Invitrogen) and quality verified using Agilent Bioanalyzer. Labeled complementary RNA (cRNA) fragments were hybridized to Affymetrix Rat GeneChip^R Expression Set 230. The differentially expressed genes were defined as those with $p < 0.05$ on t-test and log ratio of means > 1SD. MetaCore pathway analysis identified regulated genes with a cutoff threshold of 1.2-fold and $p < 0.05$. 1,575 differentially expressed genes were used as “focus genes” for pathway analysis, and the 16,036 transcripts which passed the noise filtering steps were used as reference genes. We focused on the 5 top-ranked pathways, although no pathway passed a false discovery rate filter of 0.25. Genes that were

modulated after FK506 treatment were selected from each pathway and verified by real-time quantitative PCR (qPCR). Selected genes from the NFAT pathway and MODY (Maturity Onset Diabetes of Youth) were studied by qPCR analysis.

OXPHOS Pathway Analysis

Affymetrix annotations of each of the 1,575 transcripts included information for Gene Ontology (GO), Biological Process, Cellular Component, Molecular Function, and Pathways. Genes that had either Oxidative as part of their pathway name or electron transport in the GO were selected.

Quantitative PCR

Selected genes from regulated pathways were validated by qPCR using the Roche Universal Probe Library probes (Roche Diagnostics, Indianapolis, IN). Primer/probe combinations were designed using Roche's on-line assay design center and obtained from Integrated DNA Technologies (Coralville, IA). Reactions (20 μL) were assembled using Roche TaqMan Master Enzyme and performed using Roche LightCycler 2.0 thermal cycler. Gene expression was normalized using glyceraldehyde 3-phosphate dehydrogenase (GAPDH).

Motif analysis

To answer if co-regulation of multiple genes (up- or down-regulated) could be explained by common transcription factor activity the list of differentially regulated genes from the microarray data were analyzed using Motifs Associated with Differential Expression (motifADE). The cis-regulatory elements in the promoter regions of the genes that could regulate gene expression were predicted (20) using the ExPlain tool (BioBase, Braunschweig, Germany). Over-represented transcription factor binding sites within -2000 to 100 of the start codon of regulated genes were compared to a background set of genes using a ratio cut-off of 1.5 FC and $p < 0.001$ compared to background.

Cell Respiration

Following incubation for 24, 48, 72 and 96 hr, intact cells or isolated rat islets were added to temperature-controlled, continuously stirred chambers for measurements of oxygen consumption (Oroboros Oxygraph-2k, Innsbruck, Austria). Cells were trypsinized and suspended in RPMI medium. An aliquot of the suspension was used to determine cell numbers. Cell respiration was performed in a final volume of 2 ml at a constant temperature of 37°C with stirring at 750 RPM using a stepwise titration protocol (21). Cells were added to the oxygraph chamber and allowed to equilibrate to temperature and ambient oxygen. Baseline respiration was measured in a closed chamber over 5–10 min until a stable rate of oxygen consumption was observed. State 4 respiration was measured following the addition of 1 μl oligomycin at a final concentration of 2 μg/ml. Maximal, pseudo state 3 respiration was stimulated by stepwise titration (0.05 μM) of the uncoupler carbonyl cyanide-p-trifluoromethoxyphenylhydrazone (FCCP). Respiration was measured in the presence of rotenone (0.5 μM). Oxygen consumption rates were determined from real-time plots of oxygen concentration and flux (Datlab 4, Oroboros Instruments) and were corrected for background oxygen fluxes determined experimentally for the RPMI medium.

Mitochondrial Mass and Bioenergetics

Mitochondrial mass and bioenergetics were measured using MitoTracker Green (MTG) and MitoTracker Red (MTR) probes (Invitrogen) (22, 23). Following incubation for 24, 48, 72 and 96 hr, cells or isolated islets were incubated at 37.8°C for 30 min with 100 nM MTG or MTR. Cells were washed with warmed PBS and harvested by trypsinization. After centrifugation and resuspension of cells fluorescence was measured using a microplate

reader. Fluorescence intensity was detected with λ_{ex} = 490 and λ_{em} = 516 nm. Results were normalized to cell counts. For visualization of these findings with confocal microscopy INS-1 cells in 24-well tissue culture plates were incubated with MTG after 72 hr of treatment with 50 ng/ml FK506. Final concentrations of probes in culture medium were 0.2 M and 1 M, respectively. Islets were centrifuged at 3000 rpm for 1 min and gently resuspended in pre-warmed staining solution containing the probes and incubated for 30 minutes at 37°C. Islets were pelleted by centrifugation at 3000 rpm for 1 minute and washed twice with fresh pre-warmed medium. Islet fixation was done with PBS containing 3% paraformaldehyde at room temperature for 30 minutes and washed 3 times with PBS. Stained and fixed islets were stored at 4°C until analysis. Before analysis islet suspension (0.1–0.2 ml) was transferred to glass-bottom dishes (MatTek, Ashland, MA) and images were taken using LSM510 confocal microscope (Carl Zeiss, New York, NY) and analyzed using Image J (NIH) software.

Mitochondrial DNA (mtDNA) Abundance

DNA was extracted from cells after trypsinization using a QIAamp DNA mini kit (QIAGEN, Chatworth, CA). Samples were extracted after 72 hr of treatment from each group (FK506 and DMSO). The abundance of mtDNA-encoded NADH dehydrogenase 1 gene was measured using real-time qPCR (Applied Biosystems, Foster City, CA). Results were normalized to 28S ribosomal DNA (24).

ATP/ADP Ratio

The ATP/ADP ratio was measured at 72 hr. The ATP/ADP ratio is a sensitive indicator of the mismatch between ATP production and consumption. Cellular nucleotides were extracted after suspending cells in 0.6 M HClO4-1 mM EDTA and immediate dispersion in liquid nitrogen followed by rapid thawing, centrifugation and neutralization of supernatant with 2 M K_2HCO_3. After incubation for 30 min on ice and precipitation, nucleotide concentrations were determined by HPLC (HPLC Series 1100; Hewlett-Packard, Waldbronn, Germany) using MonoQ HR 5/50 GL column (Amersham Pharmacia Biotech, Little Chalfont, Buckinghamshire, United Kingdom) and triethylamine bicarbonate (pH 8.8) as an elution buffer. ATP, ADP, GTP, and GDP levels were normalized to protein (nmol/mg protein).

Statistical Analysis

Data were summarized using mean and standard deviation for numeric variables, and counts and percents for categorical variables. Student's t-test and ANOVA were used for the comparison of means. Data were considered significant if $p < 0.05$.

Results

Impact of FK506 and CsA on INS-1 Cell Growth, Viability, Apoptosis, and Insulin Secretion

As shown in Fig. 1A treatment of INS-1 cells with 15 – 150 ng/ml FK506 resulted in a small, but significant reduction in cell number at 50 and 150 ng/ml beginning at 48 hr and reaching 20% reduction at 72 hr. INS-1 cell viability showed a larger impact beginning at 48 hr, reaching a 37% reduction at 96 hr (Fig. 1B). Cell viability was sensitive to FK506 treatment with absence of a significant dose-response relationship from 15–150 ng/ml, suggesting viability is affected at lower concentrations. Although cell viability was significantly impacted by FK506, INS-1 cell apoptosis was not affected at 50 ng/ml (Fig. 1C). Loss of INS-1 cell proliferation and viability in the absence of apoptosis indicates that FK506 disrupts cell function. FK506 treatment of INS-1 cells resulted in a marked decrease in insulin secretion beginning at 48 hr and with increasing impact up to 96 hr (Fig. 1D).

Insulin secretion was decreased 58% at 72 hr but like cell viability, did not exhibit a dose response relationship over the concentrations tested suggesting significant impacts at <15 ng/ml. CSA and FK506 at 800 ng/ml and 50 ng/ml, respectively, had a comparable impact on cell proliferation (Fig. 1E), cell viability (Fig. 1F), and insulin secretion and cell content (Fig. 1G).

Impact of FK506 impact on gene expression in INS-1 Cells

Since INS-1 cell function was significantly impacted by FK506 treatment, we performed microarray analyses to identify genes and pathways involved. Microarray experiments were performed after 48 hr of treatment with FK506 at 50 ng/ml or DMSO. Overall 2,810 genes exhibited significant difference between DMSO and FK506 groups ($p < 0.05$). Of these there were 1575, 621 and 293 genes that changed more than 1, 2, and 3 SD (corresponding to an average 1.2- 1.5-, and 1.7-fold change expression). Among the 293 genes that were regulated > 1.7-fold, 146 and 147 genes were up-and down-regulated, respectively. Mean fold change in down-regulated genes was 0.45 and for up-regulated genes was 2.38, indicating a two-fold regulation in each direction.

Using MetaCore pathway analysis, 5 top-ranked pathways were detected (Table 1). The emergence of potential alterations in ATP metabolism coupled with the finding of FK506-mediated reduction of insulin secretion as well reduced cell viability, which is mainly mediated by mitochondria (25), led us to explore mitochondrial pathways, including oxidative phosphorylation (OXPHOS) pathways. Sixty-five genes were differentially regulated with 50 being down-regulated.

NFAT and MODY pathways were differentially regulated (Hnf4α (1.2-fold), NeuroD1 (1.2-fold), Cdkn2c (0.7-fold) and Cdkn1a (0.7-fold)). Twelve genes from membrane trafficking, cytoskeleton remodeling, insulin secretion, OXPHOS and ATP metabolism pathways plus specific components of NFAT and MODY genes were verified using qPCR (Fig. 2).

MotifADE

A separate list of cis-regulatory motifs for each of the up-regulated and down-regulated genes is shown in Table 2. The presence of NFAT transcription factor among both up- and down-regulated genes suggests that this transcription factor plays an important role in mediating the effects of FK506.

Impact of FK506 on Mitochondrial Function

Polarography of cells treated with FK506 for 48 hr demonstrated decreased oxygen consumption (Fig. 3A). Oxygen consumption rates increased over time in cells, regardless of treatment, but FK506-treated cells exhibited significantly reduced rates beginning at 48 hr (30.09 vs. 22.65 at 48 hr, $p < 0.001$). The effect on oxygen consumption paralleled the observed decrease in cell viability. After addition of oligomycin, FCCP, and rotenone, we consistently observed a 28% to 30% lower oxygen flux in the FK506-treated cells at all time points ($p < 0.001$) (data not shown). We observed decreased mitochondrial mass based on decreased MTG binding starting at 48 hr (78.87 vs. 55.25, $p<0.001$) (Fig. 3B) and confirmed by confocal microscopy (Fig. 3C).

ATP/ADP and GTP/GDP Ratios

ATP, ADP, GTP and GDP content of FK506-treated INS-1 cells were not significantly lower than that of controls. There was no effect on ATP/ADP (8.6 vs. 8.4) or GTP/GDP (3.4 vs. 3.2) ratios (Fig. 3D).

Mitochondrial DNA Abundance

Mitochondrial DNA copy number was 15% lower in FK506 treated cells after 72 hours, but not significant (Fig. 3E)

Impact of FK506 on mitochondrial function in isolated rat islets

Mitochondrial bioenergetics and mass were assessed in islets with MTR and MTG binding, respectively. Mitochondrial bioenergetics was decreased by FK506 after 72 hours culture ($p<0.05$) (Fig, 3F and G). Mitochondrial mass was also decreased ($p<0.05$) (Fig, 3F and G). Rat islets cultured in FK506 at 50 ng/ml for 72 hours showed a 37% decrease in oxygen consumption; however, this difference was not significant (Fig, 3H).

Discussion

FK506 is a major component of immunosuppressive therapy after SOT but is associated with glucose intolerance and PTDM. We show that FK506 exerts negative influences on INS-1 cells, including cell proliferation, cell viability, insulin secretion, and mitochondrial bioenergetics and mass. Microarray studies indicated that FK506-induced islet dysfunction is mediated through multiple pathways, including mitochondrial biogenesis, ATP metabolism, membrane trafficking, and cytoskeletal remodeling. These effects were observed at concentrations of FK506 typically achieved after therapeutic administration. We compared the effects of CsA at therapeutically equivalent concentratons in INS-1 cells and found similar effects. The impact of CsA on mitochondrial biology has been extensively evaluated (26); thus we limited further investigation to FK506. We confirmed that the effect of FK506 on mitochondrial mass and bioenergetics had biologic relevance by evaluating these variables in isolated rat islets. The data indicate that FK506 therapy may contribute to the loss of β cell function following SOT and therefore PTDM

Although FK506 appeared to diminish apoptosis rates of INS-1 cells, this effect was not significant. This result is in agreement with a previous report that shows FK506 at concentrations comparable to therapeutic levels does not cause significant apoptosis in β cells (27). In contrast there was a significant decrease in cell proliferation and viability. Since decreased cell viability did not significantly affect apoptosis, the reduced oxidation of MMT may reflect the reduced oxidative capacity of these cells, a conclusion that is supported by direct oxygen consumption measurements. Also, decreased cell proliferation and insulin secretion, both energy-requiring processes, may be explained by defects in mitochondrial function. Our results were consistent with previous reports that showed impaired glucose-induced insulin secretion (GSIS) in humans (28) as well as rat islets (29, 30).

Based on microarray analysis, multiple pathways are altered in FK506-treated cells, including: ATP metabolism, G-protein signaling, cytoskeleton remodeling and membrane trafficking. Membrane trafficking and cytoskeleton remodeling are key regulators of cellular secretory functions and G-protein coupled receptors play a major role in the modulation of insulin secretion (31). In addition, Rab27a, which plays an essential role in vesicle docking, has two paradoxical effects; decreased GSIS and inhibition of insulin secretion from storage pools (32). Rab27a deficient mice display glucose intolerance due to defective GSIS (33). Since Rab27a was up-regulated (4-fold, $p < 0.001$) in our microarray, it is possible that reduced insulin secretion observed in our experiments represented basal, non-glucose-induced insulin secretion from stored pools. Another enzyme, GDH plays a similar role as Rab27a in the secretory response of β cell when stimulated but not at normo-caloric states (34). Our data showed that GDH is up-regulated in FK506 treated cells by 1.4-fold indicating a modest impact from this gene on reduced insulin secretion at basal non-glucose-

induced state. Moreover, up-regulation of Rac1 in our results, which was previously shown as an essential factor in GSIS also confirms this concept. Previous studies on INS-1 cells have shown that glucose stimulation increases Rac1 GTPase activity, suggesting that Rac1 is involved in the recruitment of secretory granules through the cytoskeletal network (35). Related to this, we validated that GNB4, a component of the membrane-trafficking pathway, was down-regulated >2.5-fold, indicating a major defect in insulin secretion machinery. The involvement of guanine nucleotide exchange factors (GEF) and guanine nucleotide binding proteins (GNB) is frequently described in insulin release from storage pools (36). This lends further support to the concept that FK506 may affect insulin secretion from storage pools.

MotifADE analysis identified the presence of HNF4, NFAT, PPAR and Smad3 transcription factors as being over-represented in the promoter regions of differentially regulated genes. HNF4 mutations result in the phenotype of MODY1 and HNF4 binds upstream of several genes whose expression is modified by FK506. Additionally, inducible expression of NFATc1 in β-cells has been shown to increase expression of all MODY genes (37). Because NFAT is regulated by Cnb1 and β cell specific Cnb1 knockout mice showed a phenotype of diabetes (7), diabetogenic effects of FK506 may be partly mediated through the calcineurin pathway. PPAR binding elements were frequently present upstream of both down- and up-regulated genes. We demonstrated that PGC1α, a co-activator of PPARγ and a key factor for mitochondrial biosynthesis, was down-regulated 2.5-fold in FK506-treated cells (Figure 2). Also CREB-binding protein (CBP)/p300, which is known to be the mediator of transcriptional effects of PGC1α (38), was down-regulated. Taken together, these lines of evidence suggest that insulin secretory defects induced by FK506 are mediated by several transcription factors that are involved in mitochondrial biology that may in turn affect ATP metabolism, resulting in diminished insulin secretion. Smad3 was also among the overly represented transcription factors among the differentially regulated genes. Smad3 appears to have an inhibitory role on insulin secretion, as it has been shown that small interfering RNAs to Smad3 relieve insulin transcriptional repression. Smad3-deficient mice exhibit moderate hyperinsulinemia and mild hypoglycemia as well as improved glucose tolerance and enhanced GSIS in vivo (39).

Oxygen consumption rates were lower in FK506-treated INS-1 cells and trended lower in isolated rat islets. There was a similar decline in oxygen consumption of INS-1 cells and islets with and without addition of specific inhibitors to respiratory chain complexes 1 and 4, suggesting that the observed effects on insulin secretion are not related to an effect inherent to the components of the electron transport chain and are instead associated with reduced mitochondrial mass. OXPHOS pathway analysis showed that NADH dehydrogenase is not changed significantly by FK506 suggesting that mitochondrial defects are independent of transcript levels of this gene. NADH dehydrogenase is one of the principal genes expressed by mtDNA and has a definitive role in the electron transport chain (40).

Our data indicate that mitochondrial mass is decreased after FK506 treatment in a time-dependent manner. This suggests a decline in mitochondrial protein content despite normal DNA abundance. Effects on reduced protein synthesis (translation rate of transcripts) or accelerated protein degradation could explain reduced mitochondrial protein content. Since selective increase in degradation of protein in tissues is unlikely to occur, reduced protein synthesis is likely the possible cause for reduced mitochondrial content. Calcineurin inhibitor impact on morphology of mitochondria has been investigated in other tissues. CsA has been shown to cause mitochondrial swelling and mitochondrial membrane potential changes in renal tubular cells (41, 42) and defective insulin secretion resulting from mitochondrial toxicity (43), but the effects of FK506 on mitochondrial function have not been investigated previously.

Although ATP and GTP were slightly reduced in the FK506-treated cells, no difference was seen in either the ATP/ADP or GTP/GDP ratios, suggesting that there was no functional disturbance of the mitochondria. While mitochondrial content and oxygen consumption were reduced in FK506 treated cells by 20% at 48hr, lack of ATP/ADP ratio or electron transport chain disturbances were supportive of an effect on mitochondrial mass rather than on mitochondrial function. Similarly, significant changes in mtDNA copy number were not observed upon FK506 treatment of INS-1 cells. Others have also shown that mitochondrial density is not always correlated with changes in mtDNA (44, 45). The possible reasons for discrepancy between mtDNA and mitochondrial mass could be that mtDNA synthesis changes take more time than mitochondrial protein synthesis. Additionally, it has been shown that the biogenesis of mitochondria and oxidative phosphorylation function are not linked to mtDNA because the main signals for mtDNA are from nuclear transcription factors (46).

In conclusion, our experiments demonstrate the complex effects of FK506 on cellular events that may culminate in reduced insulin secretion from islets. Pathways affected include the cytoskeleton, membrane trafficking, ATP generation and mitochondrial biology, findings that to our knowledge have not been previously described. We propose that mitochondrial dysfunction at the level of gene transcription and translation as the causes of reduced mitochondrial content and respiration. Reduced mitochondrial function likely contributes to decreased insulin secretion. Ex-vivo studies need to be repeated in an in-vivo system to translate these findings in the clinical situations. Finally, mitochondrial biology is complex and more in depth studies such as mitochondrial membrane potentials and calcium flux and measurement of translation rate of transcripts need to be performed.

Acknowledgments

We thank Dr. Frank Gonzalez, Mrs. Jan Daniels, Mrs. Jane Kahl, confocal microscopy facilities, Mr. James Tarara, Human Cell Therapy Laboratory Mayo Clinic for their help. B.A.I. was supported by NIH Grant KL2 RR084151. This publication was supported by NIH/NCRR CTSA Grant Number UL1 RR024150. Its contents are solely the responsibility of the authors and do not necessarily represent the official views of the NIH.

References

1. Dean PG, Kudva YC, Stegall MD. Long-term benefits of pancreas transplantation. Curr Opin Organ Transplant. 2008; 13 (1):85. [PubMed: 18660712]
2. Montori VM, Basu A, Erwin PJ, Velosa JA, Gabriel SE, Kudva YC. Posttransplantation diabetes: a systematic review of the literature. Diabetes Care. 2002; 25 (3):583. [PubMed: 11874952]
3. Heisel O, Heisel R, Balshaw R, Keown P. New onset diabetes mellitus in patients receiving calcineurin inhibitors: a systematic review and meta-analysis. Am J Transplant. 2004; 4 (4):583. [PubMed: 15023151]
4. Balla A, Chobanian M. New-onset diabetes after transplantation: a review of recent literature. Curr Opin Organ Transplant. 2009; 14 (4):375. [PubMed: 19542891]
5. Cosio FG, Kudva Y, van der Velde M, et al. New onset hyperglycemia and diabetes are associated with increased cardiovascular risk after kidney transplantation. Kidney Int. 2005; 67 (6):2415. [PubMed: 15882287]
6. Ueki M, Yasunami Y, Ryu S, Arima T, Ikeda S, Tanaka M. Functional and morphologic characterization of renal subcapsular islet isografts in rats treated with FK 506. Transplant Proc. 1994; 26 (2):740. [PubMed: 7513469]
7. Heit JJ, Apelqvist AA, Gu X, et al. Calcineurin/NFAT signalling regulates pancreatic beta-cell growth and function. Nature. 2006; 443 (7109):345. [PubMed: 16988714]
8. Kruger M, Schwaninger M, Blume R, Oetjen E, Knepel W. Inhibition of CREB- and cAMP response element-mediated gene transcription by the immunosuppressive drugs cyclosporin A and FK506 in T cells. Naunyn Schmiedebergs Arch Pharmacol. 1997; 356 (4):433. [PubMed: 9349628]

9. Ishizuka J, Gugliuzza KK, Wassmuth Z, et al. Effects of FK506 and cyclosporine on dynamic insulin secretion from isolated dog pancreatic islets. Transplantation. 1993; 56 (6):1486. [PubMed: 7506454]
10. Oetjen E, Baun D, Beimesche S, et al. Inhibition of human insulin gene transcription by the immunosuppressive drugs cyclosporin A and tacrolimus in primary, mature islets of transgenic mice. Mol Pharmacol. 2003; 63 (6):1289. [PubMed: 12761338]
11. Lawrence MC, Bhatt HS, Watterson JM, Easom RA. Regulation of insulin gene transcription by a Ca(2+)-responsive pathway involving calcineurin and nuclear factor of activated T cells. Mol Endocrinol. 2001; 15 (10):1758. [PubMed: 11579208]
12. Radu RG, Fujimoto S, Mukai E, et al. Tacrolimus suppresses glucose-induced insulin release from pancreatic islets by reducing glucokinase activity. Am J Physiol Endocrinol Metab. 2005; 288 (2):E365. [PubMed: 15479952]
13. Drachenberg CB, Klassen DK, Weir MR, et al. Islet cell damage associated with tacrolimus and cyclosporine: morphological features in pancreas allograft biopsies and clinical correlation. Transplantation. 1999; 68 (3):396. [PubMed: 10459544]
14. Hirano Y, Fujihira S, Ohara K, Katsuki S, Noguchi H. Morphological and functional changes of islets of Langerhans in FK506-treated rats. Transplantation. 1992; 53 (4):889. [PubMed: 1373536]
15. Plaumann S, Blume R, Borchers S, Steinfelder HJ, Knepel W, Oetjen E. Activation of the dual-leucine-zipper-bearing kinase and induction of beta-cell apoptosis by the immunosuppressive drug cyclosporin A. Mol Pharmacol. 2008; 73 (3):652. [PubMed: 18042735]
16. Laurence, L.; Brunton, JSLaKLP. Goodman & Gilman's Pharmacology. 11. McGraw-Hill Companies; 2006.
17. Fridlyand LE, Ma L, Philipson LH. Adenine nucleotide regulation in pancreatic beta-cells: modeling of ATP/ADP-Ca2+ interactions. Am J Physiol Endocrinol Metab. 2005; 289 (5):E839. [PubMed: 15985450]
18. Jensen MV, Joseph JW, Ronnebaum SM, Burgess SC, Sherry AD, Newgard CB. Metabolic cycling in control of glucose-stimulated insulin secretion. Am J Physiol Endocrinol Metab. 2008; 295 (6):E1287. [PubMed: 18728221]
19. http://www.surgery.wisc.edu/research/researchers-labs/fernandez/protocols/.
20. Mootha VK, Handschin C, Arlow D, et al. Erralpha and Gabpa/b specify PGC-1alpha-dependent oxidative phosphorylation gene expression that is altered in diabetic muscle. Proc Natl Acad Sci U S A. 2004; 101 (17):6570. [PubMed: 15100410]
21. Hutter E, Renner K, Pfister G, Stockl P, Jansen-Durr P, Gnaiger E. Senescence-associated changes in respiration and oxidative phosphorylation in primary human fibroblasts. Biochem J. 2004; 380 (Pt 3):919. [PubMed: 15018610]
22. Civitarese AE, Ukropcova B, Carling S, et al. Role of adiponectin in human skeletal muscle bioenergetics. Cell Metab. 2006; 4 (1):75. [PubMed: 16814734]
23. Agnello M, Morici G, Rinaldi AM. A method for measuring mitochondrial mass and activity. Cytotechnology. 2008; 56 (3):145. [PubMed: 19002852]
24. Short KR, Bigelow ML, Kahl J, et al. Decline in skeletal muscle mitochondrial function with aging in humans. Proc Natl Acad Sci U S A. 2005; 102 (15):5618. [PubMed: 15800038]
25. Liu Y, Peterson DA, Kimura H, Schubert D. Mechanism of cellular 3-(4,5-dimethylthiazol-2-yl)-2,5-diphenyltetrazolium bromide (MTT) reduction. J Neurochem. 1997; 69 (2):581. [PubMed: 9231715]
26. Piot C, Croisille P, Staat P, et al. Effect of cyclosporine on reperfusion injury in acute myocardial infarction. N Engl J Med. 2008; 359 (5):473. [PubMed: 18669426]
27. Hernandez-Fisac I, Pizarro-Delgado J, Calle C, et al. Tacrolimus-induced diabetes in rats courses with suppressed insulin gene expression in pancreatic islets. Am J Transplant. 2007; 7 (11):2455. [PubMed: 17725683]
28. Nielsen JH, Mandrup-Poulsen T, Nerup J. Direct effects of cyclosporin A on human pancreatic beta-cells. Diabetes. 1986; 35 (9):1049. [PubMed: 3527825]
29. Herold KC, Nagamatsu S, Buse JB, Kulsakdinun P, Steiner DF. Inhibition of glucose-stimulated insulin release from beta TC3 cells and rodent islets by an analog of FK506. Transplantation. 1993; 55 (1):186. [PubMed: 7678356]

30. Uchizono Y, Iwase M, Nakamura U, Sasaki N, Goto D, Iida M. Tacrolimus impairment of insulin secretion in isolated rat islets occurs at multiple distal sites in stimulus-secretion coupling. Endocrinology. 2004; 145 (5):2264. [PubMed: 14962991]

31. Doyle ME, Egan JM. Mechanisms of action of glucagon-like peptide 1 in the pancreas. Pharmacol Ther. 2007; 113 (3):546. [PubMed: 17306374]

32. Merrins MJ, Stuenkel EL. Kinetics of Rab27a-dependent actions on vesicle docking and priming in pancreatic beta-cells. J Physiol. 2008; 586 (Pt 22):5367. [PubMed: 18801842]

33. Kasai K, Ohara-Imaizumi M, Takahashi N, et al. Rab27a mediates the tight docking of insulin granules onto the plasma membrane during glucose stimulation. J Clin Invest. 2005; 115 (2):388. [PubMed: 15690086]

34. Carobbio S, Frigerio F, Rubi B, et al. Deletion of glutamate dehydrogenase in beta-cells abolishes part of the insulin secretory response not required for glucose homeostasis. J Biol Chem. 2009; 284 (2):921. [PubMed: 19015267]

35. Li J, Luo R, Kowluru A, Li G. Novel regulation by Rac1 of glucose-and forskolin-induced insulin secretion in INS-1 beta-cells. Am J Physiol Endocrinol Metab. 2004; 286 (5):E818. [PubMed: 14736704]

36. Kowluru A. Small G Proteins in Islet {beta}-Cell Function. Endocr Rev. 2009

37. Heit JJ. Calcineurin/NFAT signaling in the beta-cell: From diabetes to new therapeutics. Bioessays. 2007; 29 (10):1011. [PubMed: 17876792]

38. Puigserver P, Adelmant G, Wu Z, et al. Activation of PPARgamma coactivator-1 through transcription factor docking. Science. 1999; 286 (5443):1368. [PubMed: 10558993]

39. Lin HM, Lee JH, Yadav H, et al. Transforming growth factor-beta/Smad3 signaling regulates insulin gene transcription and pancreatic islet beta-cell function. J Biol Chem. 2009; 284 (18): 12246. [PubMed: 19265200]

40. Albert Lehninger, DLN.; Cox, Michael M. Lehninger Principles of Biochemistry. 5. 2008.

41. Nacar A, Kiyici H, Ogus E, et al. Ultrastructural examination of glomerular and tubular changes in renal allografts with cyclosporine toxicity. Ren Fail. 2006; 28 (7):543. [PubMed: 17050236]

42. Simon N, Morin C, Urien S, Tillement JP, Bruguerolle B. Tacrolimus and sirolimus decrease oxidative phosphorylation of isolated rat kidney mitochondria. Br J Pharmacol. 2003; 138 (2):369. [PubMed: 12540528]

43. Dufer M, Krippeit-Drews P, Lembert N, Idahl LA, Drews G. Diabetogenic effect of cyclosporin A is mediated by interference with mitochondrial function of pancreatic B-cells. Mol Pharmacol. 2001; 60 (4):873. [PubMed: 11562451]

44. Toledo FG, Menshikova EV, Ritov VB, et al. Effects of physical activity and weight loss on skeletal muscle mitochondria and relationship with glucose control in type 2 diabetes. Diabetes. 2007; 56 (8):2142. [PubMed: 17536063]

45. Morino K, Petersen KF, Dufour S, et al. Reduced mitochondrial density and increased IRS-1 serine phosphorylation in muscle of insulin-resistant offspring of type 2 diabetic parents. J Clin Invest. 2005; 115 (12):3587. [PubMed: 16284649]

46. Moraes CT. What regulates mitochondrial DNA copy number in animal cells? Trends Genet. 2001; 17 (4):199. [PubMed: 11275325]

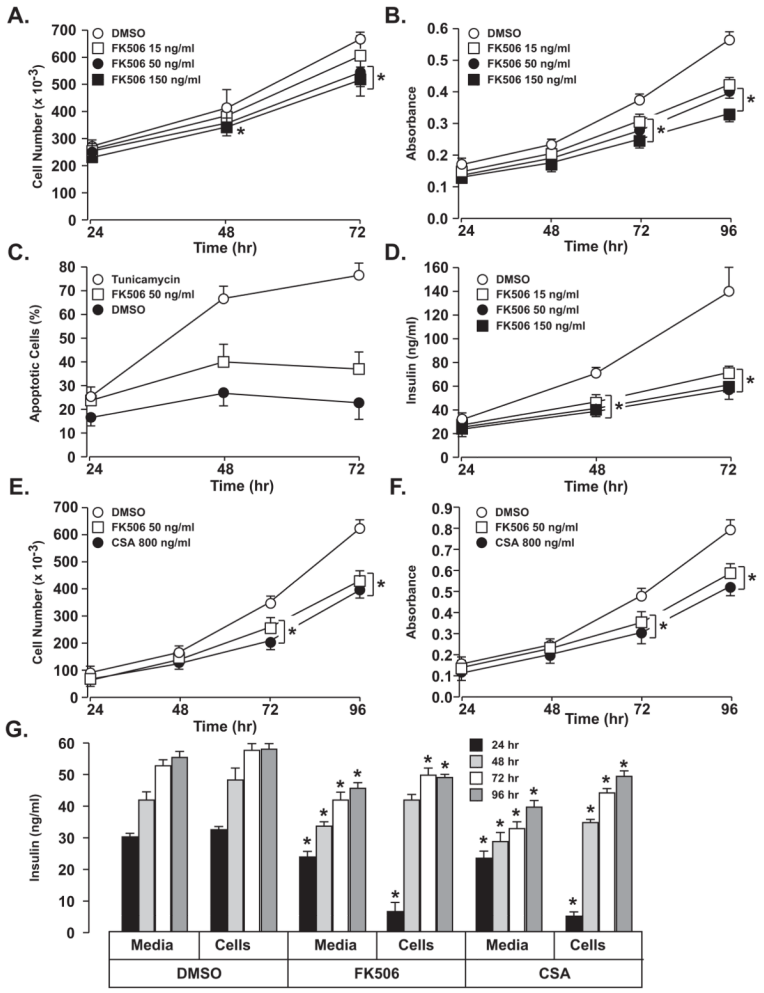

Figure 1. Impact of FK506 and CSA on INS-1 cell proliferation, cell growth (MTT assay), apoptosis and insulin secretion

Significant changes in INS-1 cell proliferation (A) and cell viability (B) were observed after FK506 treatment up to 4 days. There was not a significant change in the rate of apoptosis (C) with FK506 treatment at 50ng/ml and Tunicamycin was used as positive control. Insulin secretion was markedly reduced in INS-1 cells after FK506 treatment at different concentrations (D). Treatment of INS-1 cells with CSA at 800 ng/ml and FK506 at 50 ng/ml produced significant and comparable reductions in both INS-1 cell proliferation (E), vialbility (F), and insulin secretion and cell content (G). Values represent mean ± SEM. Asterisks shows statistically significant differences at $p < 0.05$. All Experiments were performed at least three times and in triplicate.

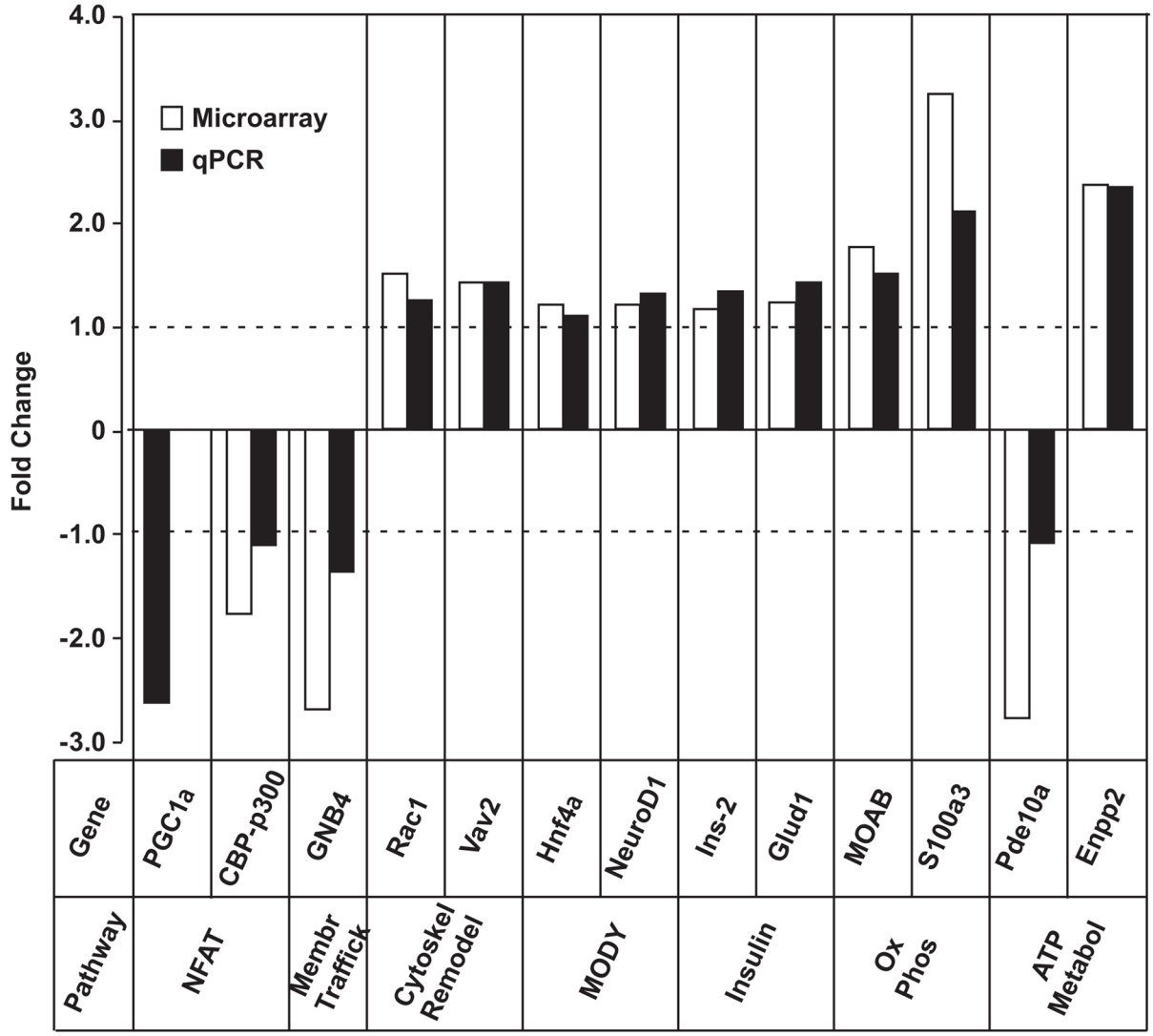

Figure 2.
Verified genes by qPCR analysis and the Log2 Fold Changes (FC) of their regulation.

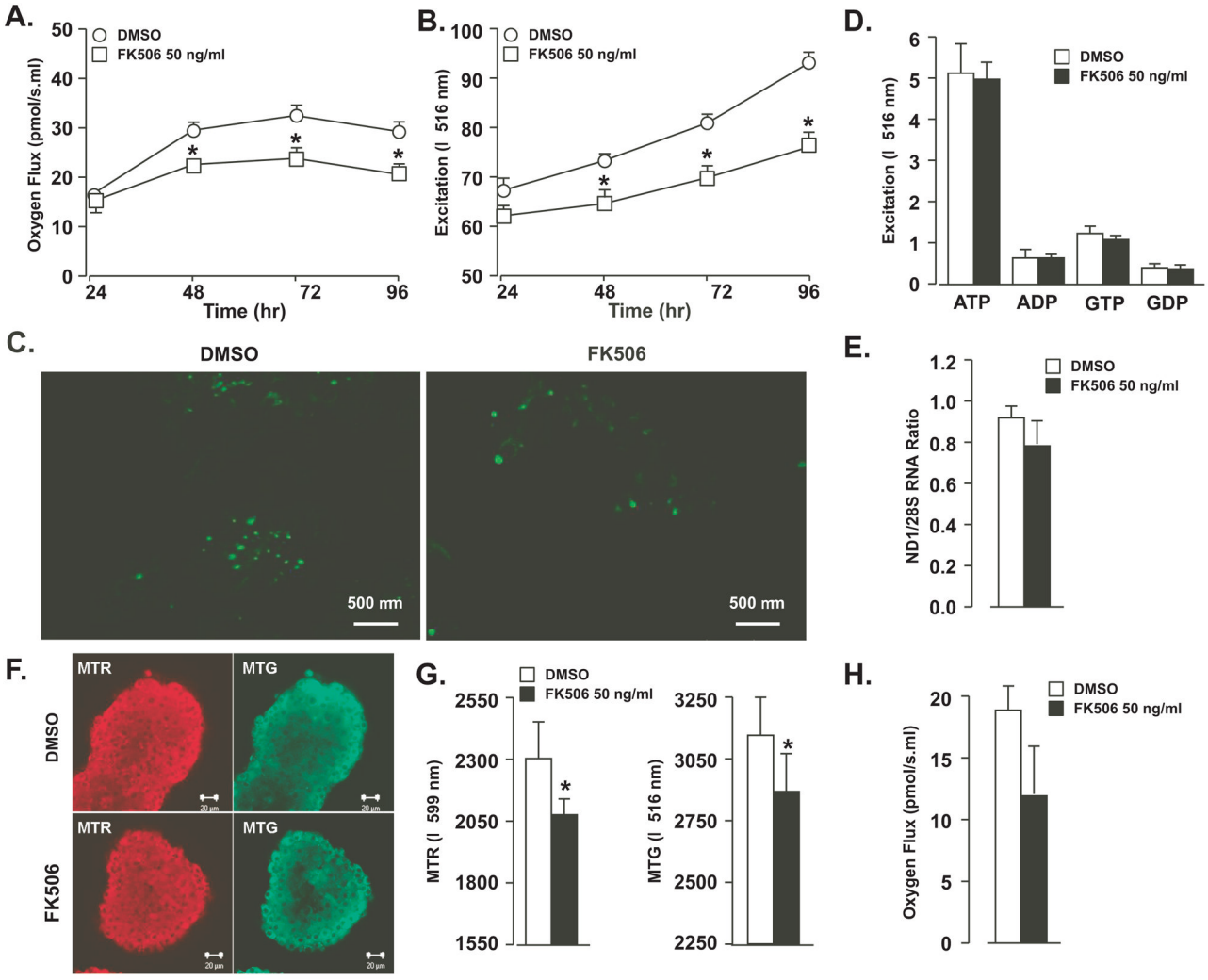

Figure 3.

Mitochondrial function and content assessment of INS-1 cells and isolated rat islets. FK506 (50 ng/ml) treatment of INS-1 cells resulted in reduced oxygen consumption (A), reduced mitochondrial mass as assessed by Mitotracker Green binding (B) and verified by confocal microscopy after mitotracker green of DMSO- and FK506-treated cells (C). The ATP/ADP and GTP/GDP ratios (D) and mitochondrial copy number (E) were unaffected by FK506 treatment. Treatment of isolated rat islets with FK506 (50 ng/ml) resulted in significant reduced mitochondrial bioenergetics and mass as assessed by Mitotracker Red and Green dye binding, respectively (F and G). FK506 (50 ng/ml) decreased oxygen consumption is rat islets by 37% after 72 hr in culture (H); however, this difference was not statistically significant ($p = 0.2$). Values represent mean ± SEM. Asterisks shows statistically significant differences at $p < 0.05$. All experiments were performed at least three times.

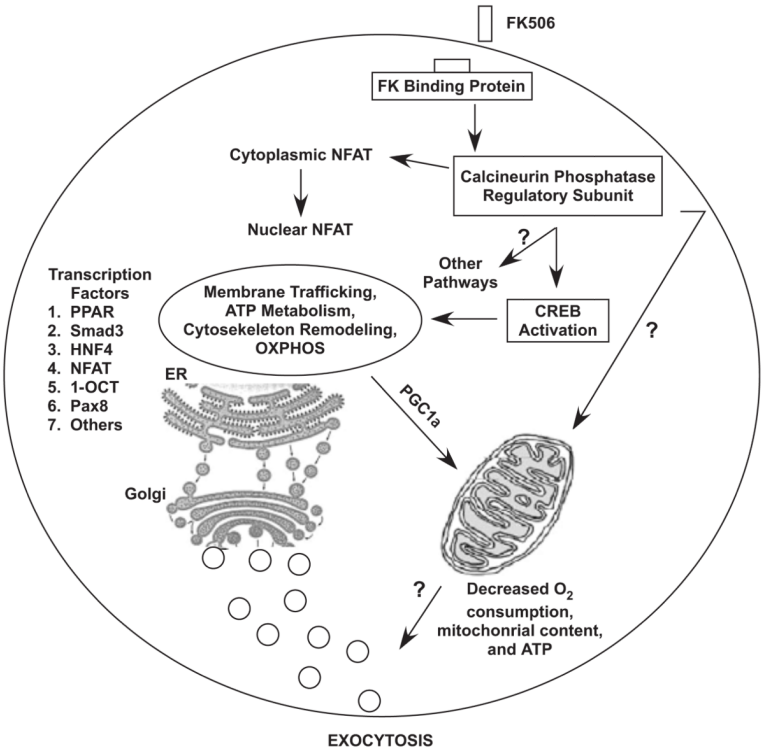

Figure 4.
Schematic representation of pathways implicated in the effect of FK506 on islet cell function.

Table 1

Pathway analysis of Microarray data showed 4 important pathways were regulated after 48 hours of FK506 treatment.

Pathway	Regulated genes	FC	p-value
Cytoskeleton remodeling	Neuroepithelial cell-transforming gene 1 protein	1.28	0.01
	Serine/threonine-protein kinase PAK 1	1.34	<0.01
	Platelet-derived growth factor A chain precursor	0.72	<0.01
	Phosphatidylinositol 3-kinase regulatory subunit alpha	1.28	0.01
	Ras-related C3 botulinum toxin substrate 1 precursor	1.49	0.02
	T-lymphoma invasion and metastasis-inducing protein 1	0.6	<0.01
	Protein vav-2	1.4	0.04
Transport Membrane trafficking	Guanine nucleotide-binding protein G(i), alpha-2 subunit	1.2	<0.01
	Guanine nucleotide-binding protein subunit beta-4	0.37	<0.01
	Guanine nucleotide-binding protein G(I)/G(S)/G(O) subunit γ-12 prec.	1.19	0.02
	Guanine nucleotide-binding protein G(I)/G(S)/G(O) subunit γ-3 prec.	0.56	0.01
	Guanine nucleotide-binding protein G(I)/G(S)/G(O) subunit γ-7 prec.	0.74	<0.01
	1-phosphatidylinositol-4,5-bisphosphate phosphodiesterase beta-4	1.21	<0.01
	Rap1 GTPase-activating protein 1	1.34	<0.01
G-protein signaling G-Proteins mediated regulation p38 and JNK signaling	B-cell linker protein	2.23	<0.01
	Guanine nucleotide-binding protein G(i), alpha-2 subunit	1.21	<0.01
	Guanine nucleotide-binding protein subunit beta-4	0.37	<0.01
	Guanine nucleotide-binding protein G(I)/G(S)/G(O) subunit γ-12 prec.	1.19	0.02
	Guanine nucleotide-binding protein G(I)/G(S)/G(O) subunit γ-3 prec.	0.56	0.01
	Guanine nucleotide-binding protein G(I)/G(S)/G(O) subunit γ-7 prec.	0.74	<0.01
	Dual specificity mitogen-activated protein kinase kinase 6	1.43	<0.01
	Mitogen-activated protein kinase 10	0.76	0.02
	Serine/threonine-protein kinase PAK 1	1.33	0.02
	1-phosphatidylinositol-4,5-bisphosphate phosphodiesterase beta-4	1.21	0.001
	Protein tyrosine kinase 2 beta	1.99	<0.01
	Ras-related C3 botulinum toxin substrate 1 precursor	1.49	0.02
	Protein vav-2	1.4	0.04
ATP metabolism	Ectonucleotide pyrophosphatase/phosphodiesterase (member 2) prec.	2.36	<0.01
	Ectonucleotide pyrophosphatase/phosphodiesterase family member 3	1.63	<0.01
	Ectonucleoside triphosphate diphosphohydrolase 3	1.22	0.04
	phosphodiesterase 10A	0.36	<0.01
	cGMP-dependent 3′,5′-cyclic phosphodiesterase	0.57	<0.01
	cGMP-inhibited 3′,5′-cyclic phosphodiesterase B	1.31	<0.01
	cAMP-specific 3′,5′-cyclic phosphodiesterase 4B	0.51	<0.01
	cAMP-specific 3′,5′-cyclic phosphodiesterase 4C	0.76	0.03
	phosphodiesterase 8A	0.54	0.01

Pathway	Regulated genes	FC	p-value
	Tryptophanyl-tRNA synthetase, cytoplasmic	1.18	<0.01

Table 2

MotifADE analysis showing the highly frequent transcription factors in the cis-regulatory motifs upstream of regulated genes.

Transcription factor	Frequency ratio for down-regulated genes	Transcription factor	Frequency ratio for up-regulated genes
PPAR	1.8871	SREBP	1.7203
PPARA	1.7833	PAX5	1.6671
SMAD3	1.754	NFKB	1.6585
CREB	1.6376	SMAD3	1.6064
TAXCREB	1.5875	PAX4	1.591
GATA	1.531	CEBP	1.5795
STAT	1.4206	SOX9	1.5643
NFAT	1.4976	PPAR	1.539
GATA4	1.4846	PPARA	1.5227
HNF4	1.4184	TAXCREB	1.4756
CEBP	1.4178	1-Oct	1.469
SOX9	1.4053	HNF1	1.4643
GATA	1.2469	STAT1	1.4605
TTF1	1.2329	NFAT	1.4499
PAX8	1.1691	HNF6	1.4484
PAX5	1.1569	CEBPA	1.4294
PAX3	1.1442	OCT	1.3967
CEBPGAMMA	1.1417	GATA4	1.3431
PAX2	1.1222	PAX8	1.2882